

WAVEFRONT SENSING AND ADAPTIVE OPTICS IN VISIBLE RANGE

Pascal Mercère^(2,3), Thomas.A. Planchon⁽¹⁾, Gilles Chériaux⁽¹⁾, Jean-Paul Chambaret⁽¹⁾, Philippe Zeitoun^(1,2),
Xavier Levecq⁽³⁾, Guillaume Dovillaire⁽³⁾

(1) - Laboratoire d'Optique appliquée, ENSTA - Ecole Polytechnique, Chemin de la Hunière, 91761
Palaiseau Cedex - France

(2) - Laboratoire de Spectroscopie Atomique et Ionique, Bât. 350, Université Paris-Sud, 91405 Orsay -
France

(3) - Imagine Optic, 18 rue Charles De Gaulle 91400 Orsay - France

Abstract :

This paper relates experiences we have recently realised at the Laboratoire d'Optique Appliquée. Our aim was firstly to correct a strongly phase-distorted laser beam, secondly estimate the limits of our instruments. The analyses were performed with the Shack-Hartmann wavefront sensor (SHWS) developed by Imagine Optic company. The advantage of using such a sensor leads in the simultaneous measurement of both intensity distribution and phase distortion of the optical field.

Comparison between real focal spot and the one deduced from SHWS measurement shows a good agreement.

I - Introduction

Currently, SHWS is one of the most well-known and widely used wavefront sensor. It gives in real time highly accurate measurements of both intensity distribution and phase distortion of optical fields. Essential parameters for wavefront analysis, such as Peak-to-Valley (PV), root-mean square (rms), Zernike coefficients and Strehl ratio, can be easily calculated from experimental data.

Also its compactness and versatility make this type of sensor readily usable in lots of various optical systems.

II - Principle of the Shack-Hartmann wavefront sensor

SHWS estimates the wavefront local slopes by sampling many sub-apertures of an incoming beam. This sampling is obtained by using a microlenslet array, which focuses the beamlet onto the sensitive part of a CCD camera (*Figure 1*). Thus, each sub-aperture of the lenslet array provides its own spot on the CCD camera and the sensor output is a set of $\{x,y\}$ spot centroid positions (Hartmann pattern). A locally plane

wavefront will be focused on the optical axis of the microlens, while a locally tilted one will be focused outside (above or under the axis depending on the tilt angle).

So, the local derivative of the wavefront is given by $\tan(\alpha) = \Delta x/f$, where α is the tilt angle, Δx (or Δy in the other dimension) the distance between the spot centroid position and the optical axis, and f the focal length of the microlenses. The whole wavefront is obtained by simple integration of the local slopes.

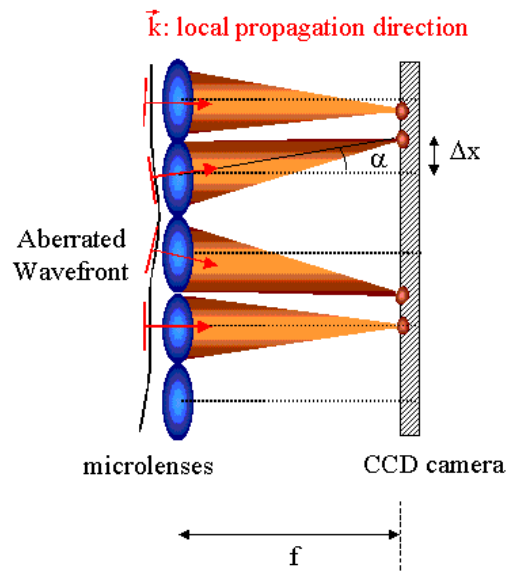


Figure 1: Principle of the Shack-Hartmann wavefront sensor

Reconstruction quality depends on the number of microlenses the incident wavefront is decomposed by. Higher this number, more accurate results will be obtained. Of course, the numerical method used for integration is also essential in the experimental data treatment.

The wavefront reconstruction is called either *zonal* or *modal*, depending on whether the phase is presented like a number of local slopes or in terms of coefficients of a modal function (Zernike polynomials for circular pupils or Legendre polynomials for square pupils). The modal reconstruction is very useful because the coefficients we access to, have a real physical sense and represent the optical aberrations commonly known as tilt, focus, astigmatism or coma. However restrictions subsist. The use of modal reconstruction algorithms implies to work on a particular pupil geometry (the software determines the largest circular or square pupil on the incident wavefront) and the projection onto a finite number of polynomials generates a spatial filtering.

III – Experimental set-up

The experiment was performed with a cw Ti:Sa laser ($\lambda \approx 800\text{nm}$) pumped by a tunable Argon laser used at $\lambda \approx 500\text{nm}$. Working parameters were as followed:

- Argon pump laser 5.7 W
- Ti:Sa laser 1.3 W exit power after optimisation

In the first part of the assembly, a spatial filter pinhole ($\Phi=10\mu\text{m}$), placed at focal distance of a focusing lens, generates an incident plane wave with a relatively good wavefront. This plane wave is sent onto the deformable mirror by several plane mirrors, all placed at 45° of the optical axis to infer minimum aberrations.

The second part of the setup consists then to realize, by an appropriated lenses conjugation, an image of the deformable mirror plane onto the wavefront sensor pupil (this relay image is essential for keeping the deformable mirror linear characteristic onto the closed loop). The beam is focused by a spherical mirror of 400mm curvature radius, working in an off-axis configuration. A set {half wave plate – Glan-Taylor polariser} placed upstream the SHWS enables us to recover a part of the incident beam to focus it on a CCD camera. The focal spot image made by the CCD camera presents two major interests for our closed loop validation. First, it enables us to follow in real time the correction of the wavefront. Secondly it gives us a reference image of the focal point, to which we can compare the reconstructed image given by the SHWS.

The whole experimental setup is represented on Figure 2, and some pictures are given Figure 3.

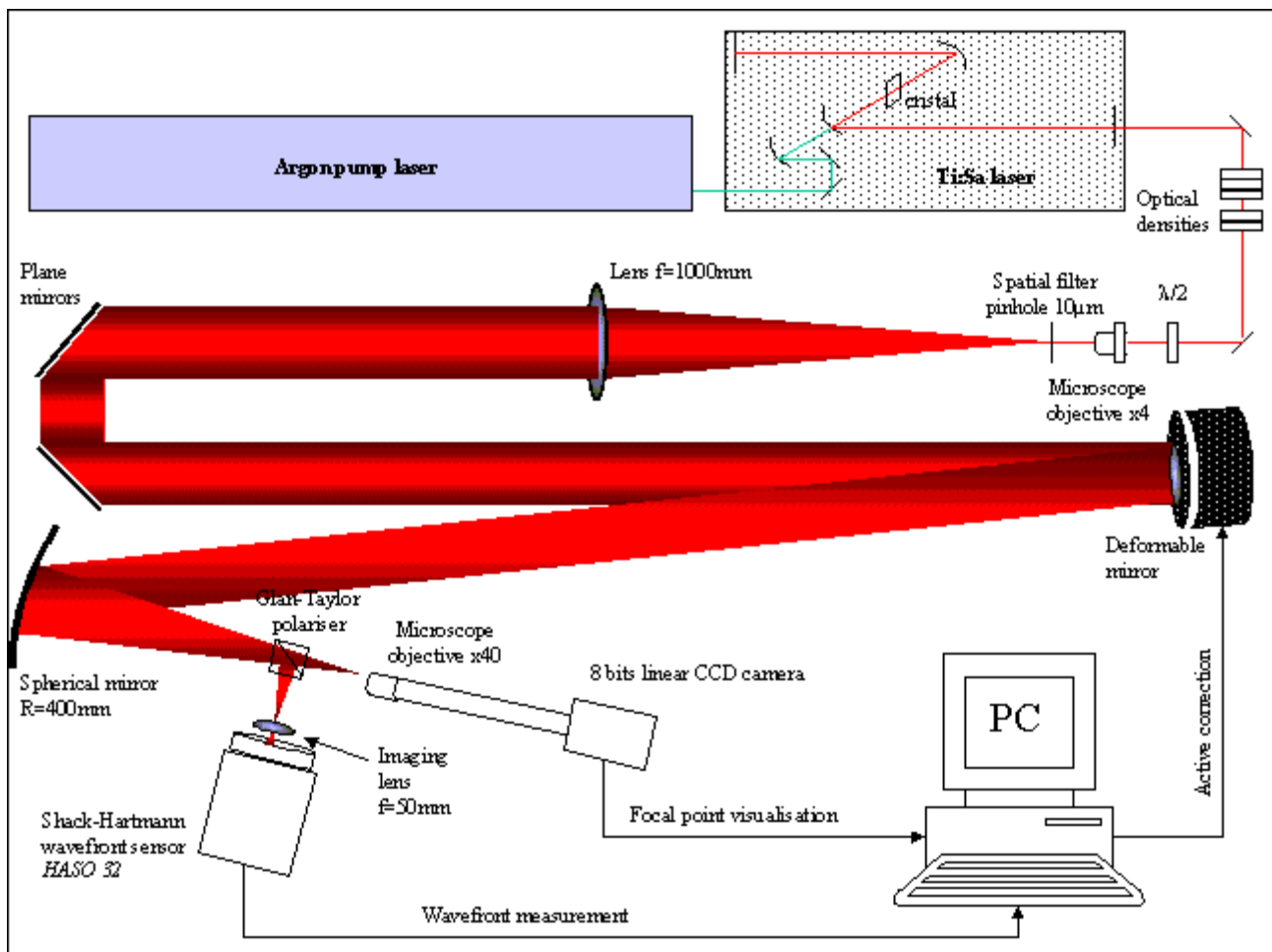


Figure 2 : The experimental setup

IV - Results

1 – Measurement of the aberrated wavefront

After having verified the relay image between the deformable mirror and the sensor pupil, a first measurement of the aberrated wavefront was performed. Figure 4 shows the intensity and phase distribution of the wavefront. We can notice the uniformity of the intensity diagram and the strong aberrations generated by the spherical mirror.

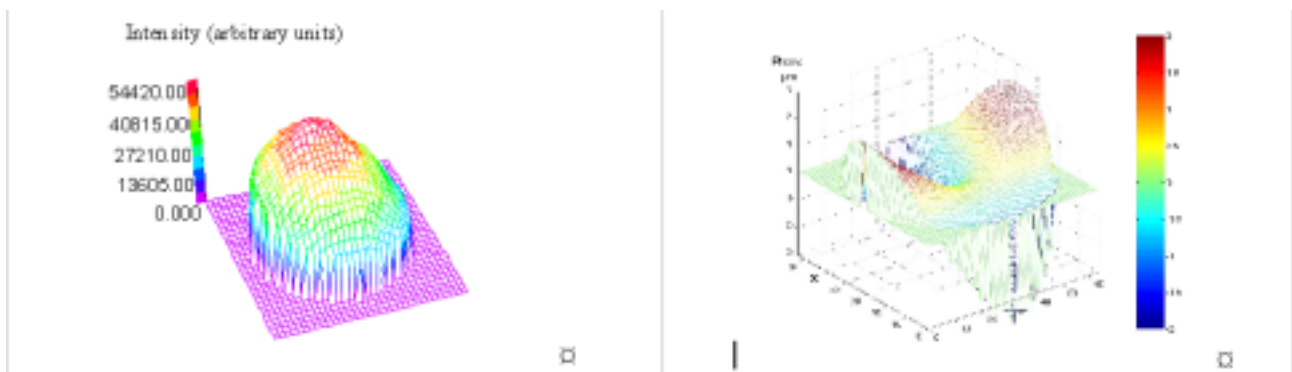


Figure 4 : 3D representations of the aberrated wavefront intensity distribution (left) and phase distortion (right)

On Figure 5, are given the different values of Zernike coefficients. As we could expected, astigmatism and coma aberrations are dominant.

Peak-to-valley and root-mean square are:

PV = 6.396 μm
rms = 1.162 μm

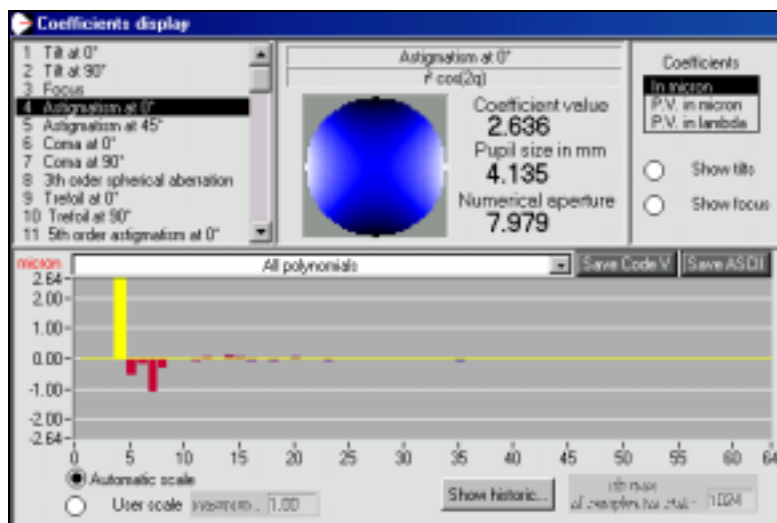


Figure 5 : Zernike coefficients before wavefront correction

On the following figure are represented the intensity and phase distributions of the measured wavefront, the corresponding Point Spread Function (PSF), as well as the Strehl ratio calculated in relation to a reference wavefront of same intensity distribution but free of phase distortions. Strehl ratio, which corresponds to the measured and reference wavefront PSF_{max} ratio, represents the quality of our optical system. It is here 0.03 before correction; so we have got, as wanted, an initially very aberrated wavefront.

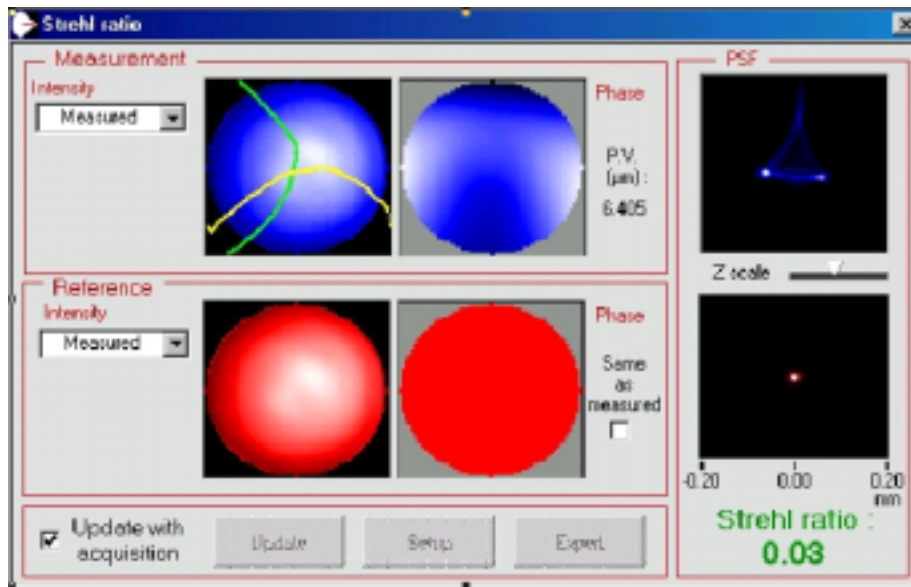


Figure 6 : Strehl ratio before wavefront correction

2 – Wavefront correction

The deformable mirror, which the closed loop was realised with, is a BIM31 CILAS bimorph mirror, composed of 31 actuators. The applied tensions can reach +/- 400V. The maximum inferred displacement is 20µm peak to valley for defocus mode, which corresponds to a mirror curvature radius of 35m. Its flatness can reach 10nm rms, its rugosity is less than 1nm rms and its reflectivity more than 96% for $0.6\mu\text{m} < \lambda < 15\mu\text{m}$. The wavefront obtained after correction is represented below:

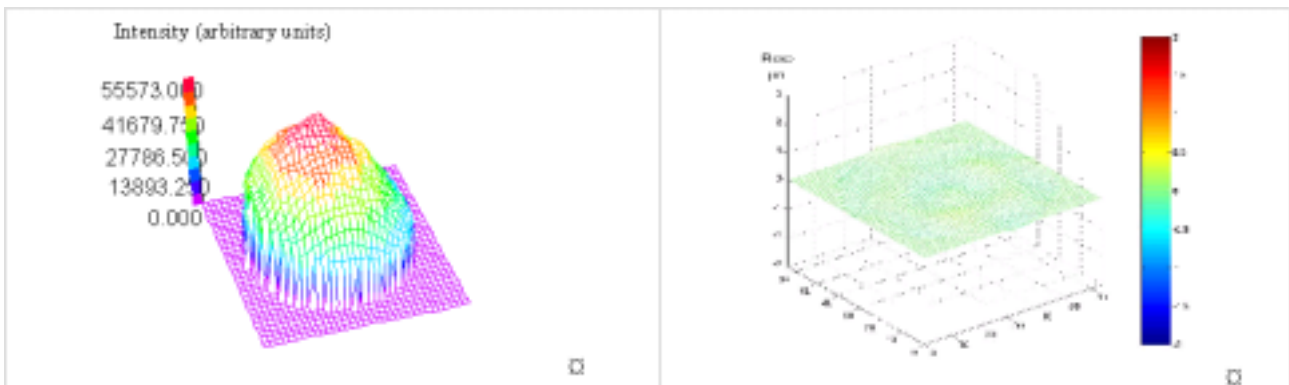


Figure 7 : 3D representations of the corrected wavefront intensity (left) and phase (right) distributions

As we can see on figure 7 and also figure 8, the aberrations of astigmatism and coma inferred by the spherical mirror are almost corrected. Only a small amount of higher order aberrations remain. PV and rms are both divided by a factor 20 after correction.

PV = 0.297 μm
rms = 0.052 μm

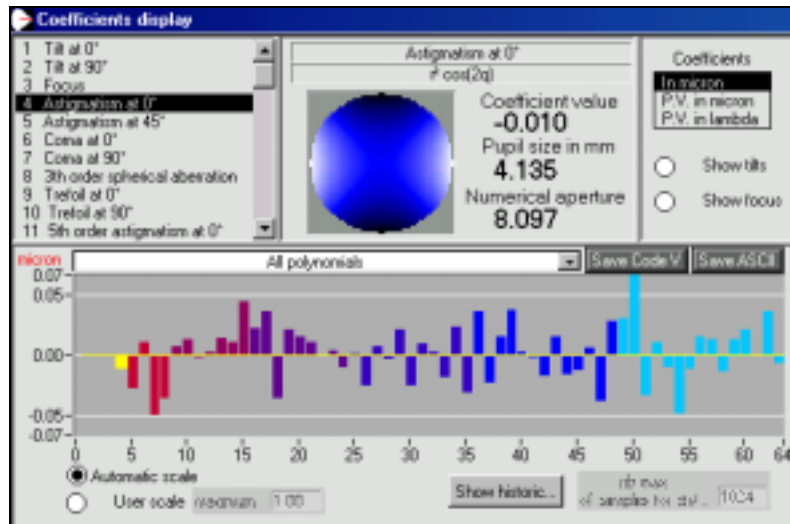


Figure 8 : Zernike coefficients after wavefront correction

Strehl ratio is now 0.85, instead of 0.03 before wavefront correction. (Figure 9)

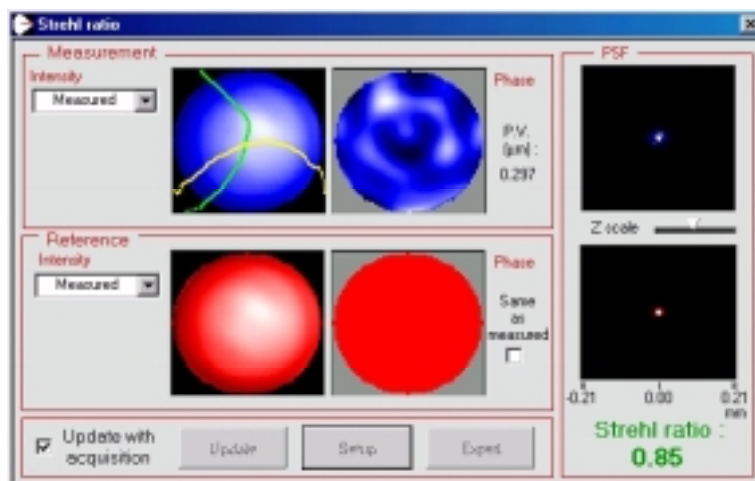


Figure 9 : Strehl ratio after wavefront correction

Note :

The tensions applied on the deformable mirror different actuators have never exceeded +/- 200V, while the closed loop was working. Tensions up to +/- 400V can be applied.

3 – Focal point imaging and Point Spread Function

The focal spot image is obtained by using an 8 bits linear CCD camera and a well-adapted microscope objective (*20 and *40 magnifications were used).

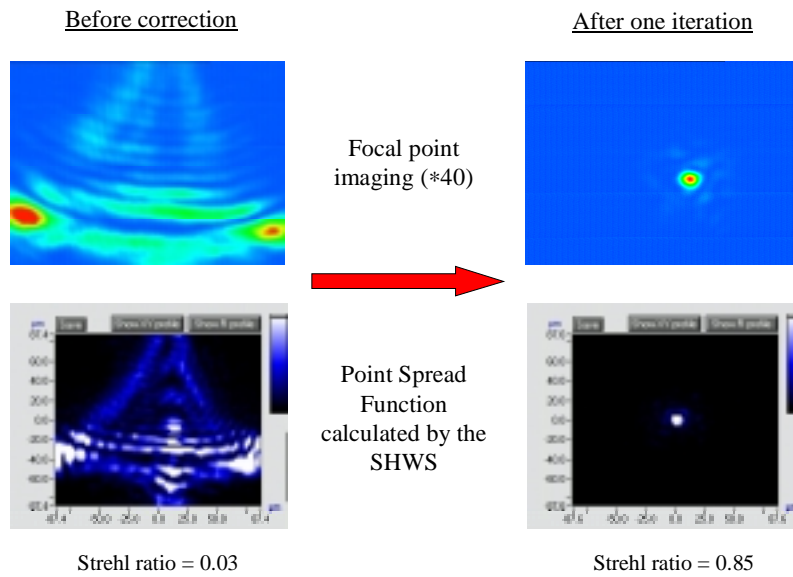


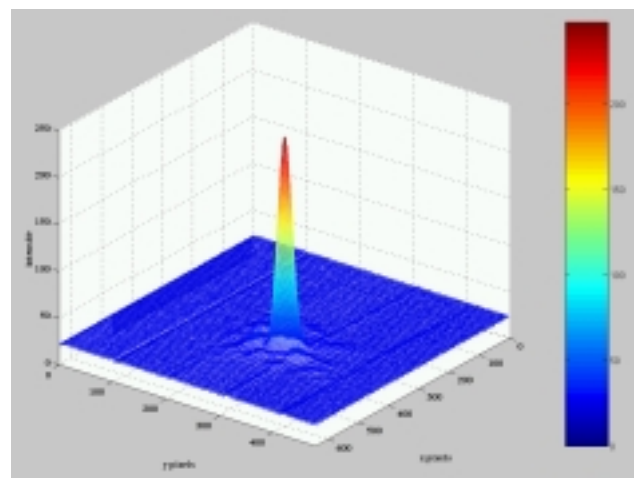
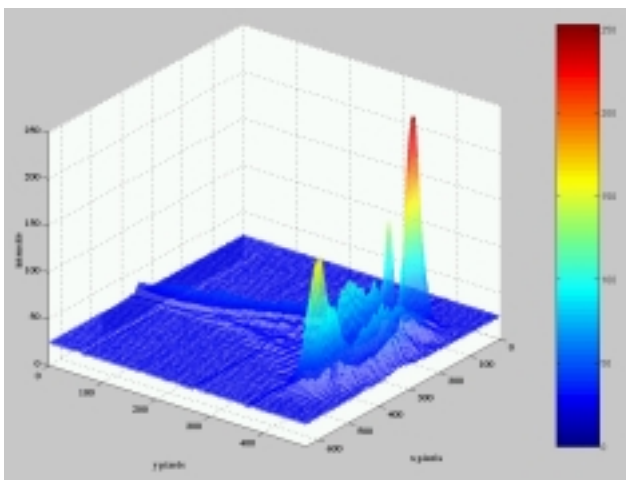
Figure 10 : Focal point – before and after correction – seen by the CCD camera and calculated by the SHWS

We can note a very good agreement between the results obtained by the two diagnostics. The dimensions of the focal point after correction are $14,736 \mu\text{m}$ at $1/e^2$ and $7,625 \mu\text{m}$ at FWHM. Diffraction limit is $7,098 \mu\text{m}$. The corresponding 3D representations are given below.

Note : Since the CCD image before correction, shown precedently and obtained with a (*40) microscope objective, is strongly saturated; we preferred to replace it by a non-saturated one obtained with a (*20) microscope objective. That have to be taken into account for comparative studies of the results!

BEFORE CORRECTION

AFTER ONE ITERATION



CCD image - objective (*20)

CCD image - objective (*40)

V- Conclusion

To correct a strongly phase-distorted cw Ti:Sa laser beam, we realised a closed loop with a Shack-Hartmann wavefront sensor and a deformable bimorph mirror. A CCD camera was used to compare the real focal spot with the one deduced from SHWS measurement.

The wavefront correction enables us to reduce the PV and rms values by a factor 20 and to increase the Strehl ratio from 0.03 before correction, up to 0.85 after correction. We could also observe a very good agreement between the focal spot images given by the SHWS and the CCD camera.

Finally, we have measured a spot diameter extremely close to the diffraction limit.